JOURNAL OF MATERIALS SCIENCE 15 (1980) 1469–1477

Deformation behaviour of single crystals of InP in uniaxial compression

G. T. BROWN, B. COCKAYNE, W. R. MACEWAN
Royal Signals and Radar Establishment, St Andrews Road, Malvern, UK

The deformation characteristics of indium phosphide (InP) single crystals under uniaxial compression have been examined as a function of strain rate, temperature and orientation. It has been shown that at temperatures below $0.55T_m$ (T_m = melting point; 1335 K) the material fractures in a brittle manner whereas at higher temperatures, within the range 0.55 to $0.71T_m$, plastic deformation occurs by both slip and deformation twinning; above $0.71T_m$, slip alone is the operative deformation mechanism. The observed operative slip systems are of the type $\{1\,1\,1\}\langle 0\,1\,1\rangle$ which are characteristic of most Group IIIb–Group Vb compounds. Deformation twinning occurs predominantly on $\{1\,1\,1\}$ planes but some activity is also observed on planes of the type $\{3\,4\,5\}$.

1. Introduction

Indium phosphide is a direct gap IIIb–Vb compound semiconductor with an energy gap of approximately 1.35 eV and is of current interest because it exhibits useful properties in microwave device applications such as amplifiers and oscillators based on the transferred electron effect, in field effect transistors and in opto-electronic devices for the 1.1 to 1.3 μm region. The fabrication of these devices requires the deposition of epitaxial layers of the same or related compounds on bulk-grown substrate material so that specific dopant profiles can be produced in the active region of the device. The presence of twins and/or dislocations in the bulk single crystals is a common problem which can restrict the usefulness of InP in these applications. For instance, twins limit the yield of uniformly orientated substrate material whilst the propagation of dislocations from the substrate into the epitaxial layers can induce defects which impair the device potential of the layer. Despite the recognized importance of twins and high dislocation densities, the deformation behaviour of InP has, hitherto, received scant attention, in marked contrast to some of the other IIIb–Vb compounds with the sphalerite (zinc blende) structure [1–4].

The sphalerite structure can be considered as two interpenetrating face-centred cubic lattices in which dislocations can glide on $\{1\,1\,1\}$ planes with a Burgers vector of $a/2\langle 0\,1\,1\rangle$. It is also believed that these dissociate into Shockley partials with Burgers vectors of the type $a/6\langle 1\,1\,2\rangle$ [5]. The stacking fault separating these Shockley partials creates a wurtzite stacking sequence across the slip plane which is identical to the stacking sequence that occurs across a coherent twin boundary on a $\{1\,1\,1\}$ plane. The energy associated with such a stacking fault, which has been determined by direct measurement of Shockley partial separation, is known to be lower for InP than for the other IIIb–Vb compounds investigated [6]. It can be concluded, therefore, that twinning is likely to occur more readily in InP than the other IIIb–Vb compounds.

Deformation twinning has been observed in the elemental semiconductors and some of the IIIb–Vb compounds [7, 8] but only in hardness tests at elevated temperatures produced with a diamond pyramid indenter. Hardness testing generates a complex distribution of stress beneath the indenter which approximates to hydrostatic compression with a superimposed shear stress. Hydrostatic compression may inhibit the onset of fracture and plastic deformation may therefore occur at temperatures lower than would be expected for testing techniques where the stress distribution does not incorporate hydrostatic compression. Clearly the

0022–2461/80/061469–09$02.90/0

TABLE I The specimens with ⟨100⟩ compression axis were cut from an undoped crystal grown on a ⟨001⟩ axis and those with the ⟨123⟩ axis were cut from an undoped crystal grown on a ⟨111⟩ axis. Both crystals were *n*-type semiconductors

Deformation axis	Etch pit density* (cm^{-2})	Carrier concentration (cm^{-3})	Mobility ($cm^2\ Vsec^{-1}$)		Resistivity (Ω cm)	
			300 K	77 K	300 K	77 K
⟨100⟩	5.8×10^4	3×10^{15}	5204	40651	0.37	0.055
⟨123⟩	2.3×10^5	4×10^{15}	4996	31077	0.28	0.055

*EPD refers to a (111)P slice.

deformation structure produced by hardness testing is not comparable to the structure produced by a simpler stress distribution and certainly the temperature dependence could be misleading. Deformation twinning has not been reported in InP although twins are a common feature of crystals grown either by the horizontal gradient freeze or liquid encapsulated Czochralski (LEC) techniques.

The present study was undertaken to examine the deformation behaviour of InP single crystals under uniaxial compression as a function of temperature, strain rate and orientation and to determine whether or not deformation twinning can occur.

2. Experimental procedure

The specimens for compression (8 mm × 3 mm × 3 mm rectangular based prisms) were prepared from undoped single crystals grown by the LEC technique in conjunction with automatic diameter control [9]. Two different compression axes were studied, ⟨001⟩ and ⟨123⟩ for which specimens were cut using a diamond saw from crystals with ⟨001⟩ and ⟨111⟩ growth axes, respectively. The data characterizing these crystals are listed in Table I; the etch pit densities were determined using a $2HCl:1HNO_3:0.25\ Br_2$ etchant [10] but the values tabulated are probably not strictly comparable because although they were both determined on slices perpendicular to the growth direction, they were cut from crystals with different growth axes.

The faces of the specimens with the ⟨001⟩ compression axis were cut parallel to {011} planes whilst those with the ⟨123⟩ axis were cut parallel to {145} and {111} planes. This facilitated the identification of the operative slip planes. Work damage was removed by free-etching the samples in a solution of a few drops of bromine in methanol with subsequent chemical polishing on synthetic flock sprayed pads soaked in the same solution. The compression testing was performed in air using an Instron Universal testing machine. The specimens were contained within a platinum resistance furnace and were heated over a period of approximately 15 min followed by stabilisation for a further 10 min; the testing temperature was controlled to ± 5° C. The scanning electron microscopy was carried out using a Cambridge Steroscan 150 instrument in the secondary electron imaging mode under an accelerating voltage of 40 kV.

Specimens for transmission electron microscopy were prepared by grinding the deformed specimens to a thickness of approximately 500 μm with subsequent chemical polishing for a further 400 μm to remove ensuing work damage. From these, 3 mm diameter discs were trepanned ultrasonically and polished chemically from both sides in a 2 vol% Br_2: 98 vol% methanol solution. Transmission electron microscopy was carried out using both a high-voltage AEI-EM7 electron microscope (HVEM) and a JEOL-100C electron microscope; the higher penetration of the former being used to examine as large an area as possible and the latter being used principally for its higher definition and selected-area diffraction capability. It was found that it was possible to use accelerating voltages as high as 800 kV in the HVEM without apparent radiation damage provided that the cold stage was utilized with a specimen temperature of approximately 150 K.

3. Results and discussion

3.1. The stress–strain relationship

Shear stress versus shear strain curves are given in Fig. 1 for specimens tested in a ductile temperature regime. These show distinct load drops which increased in magnitude for increased strain rate and also illustrate that the work hardening rate is greatly enhanced for the multiple slip orientation (Fig. 1b). Similar load drops have been reported for the deformation of GaAs [1]. This type of behaviour is known as Johnston–Gilman yielding after their original observation of this behaviour in

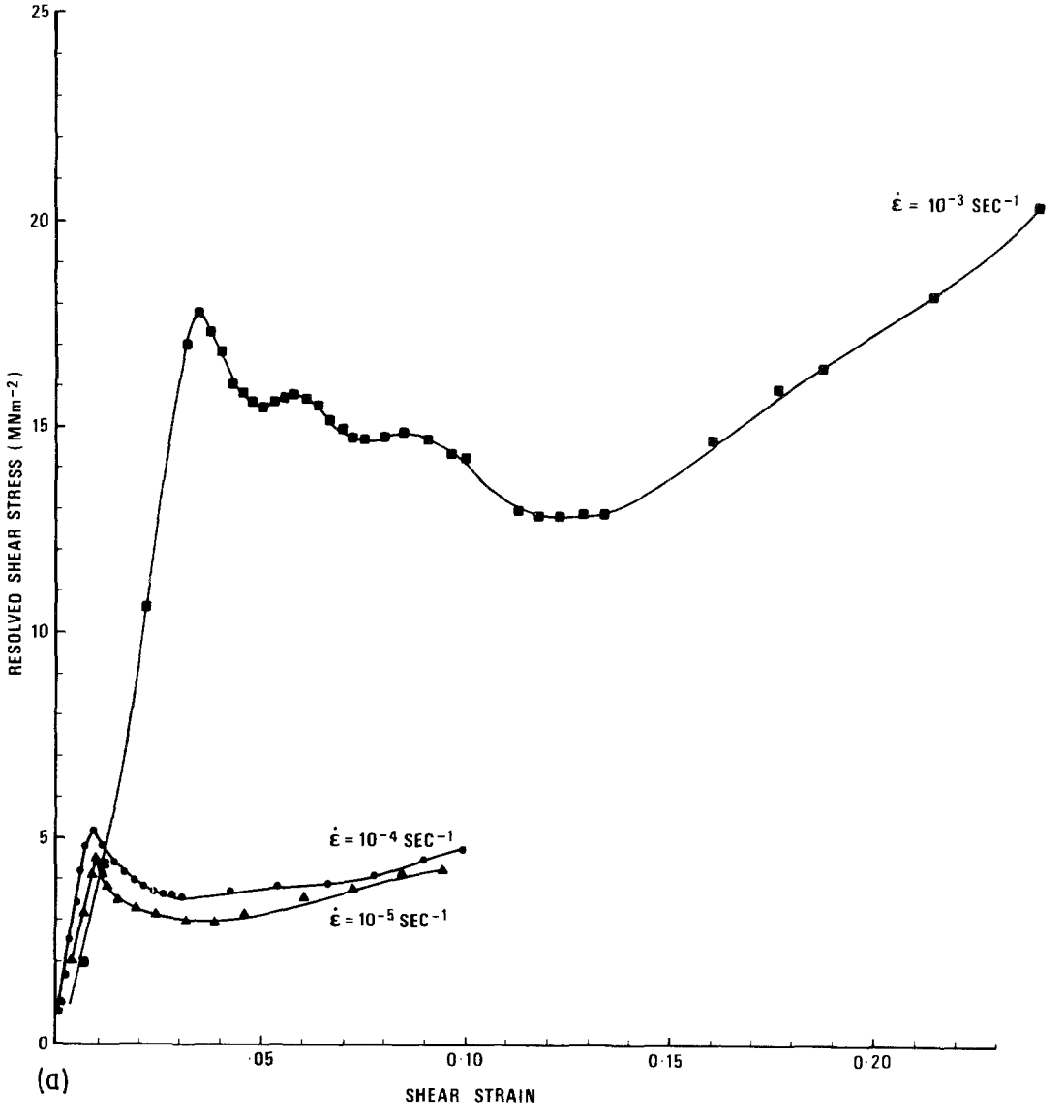

Figure 1 Resolved shear stress plotted against resolved shear strain for single crystals with (a) ⟨1 2 3⟩ axis at $0.67T_m$, (b) ⟨0 0 1⟩ axis at $0.71T_m$.

LiF [11]. Unlike the classical theory of discontinuous yielding, which is related to the stress required to unlock dislocations from their impurity atmospheres [12], the Johnston–Gilman load drop is related to the effect of stress on dislocation velocity. Prior to the upper yield point, the dislocation density and velocity are expected to increase with stress until a density is reached at which the strain rate may be accommodated by moving this dislocation density at a lower velocity. Consequently a load drop occurs, since dislocation velocity (v) is related to the applied stress (τ) by the relationship $v \propto \tau^m$ where m is a constant greater than unity.

The magnitude of the upper yield point and the load drop are a sensitive function of the initial dislocation density. For this reason samples deformed at the same temperature were extracted from the same central part of the crystal since it is known that the dislocation density may vary radially across Czochralski grown crystals [13], being greatest near to the circumference. However, the upper yield point and load drop also depend on the strain rate which is clearly illustrated in Fig.

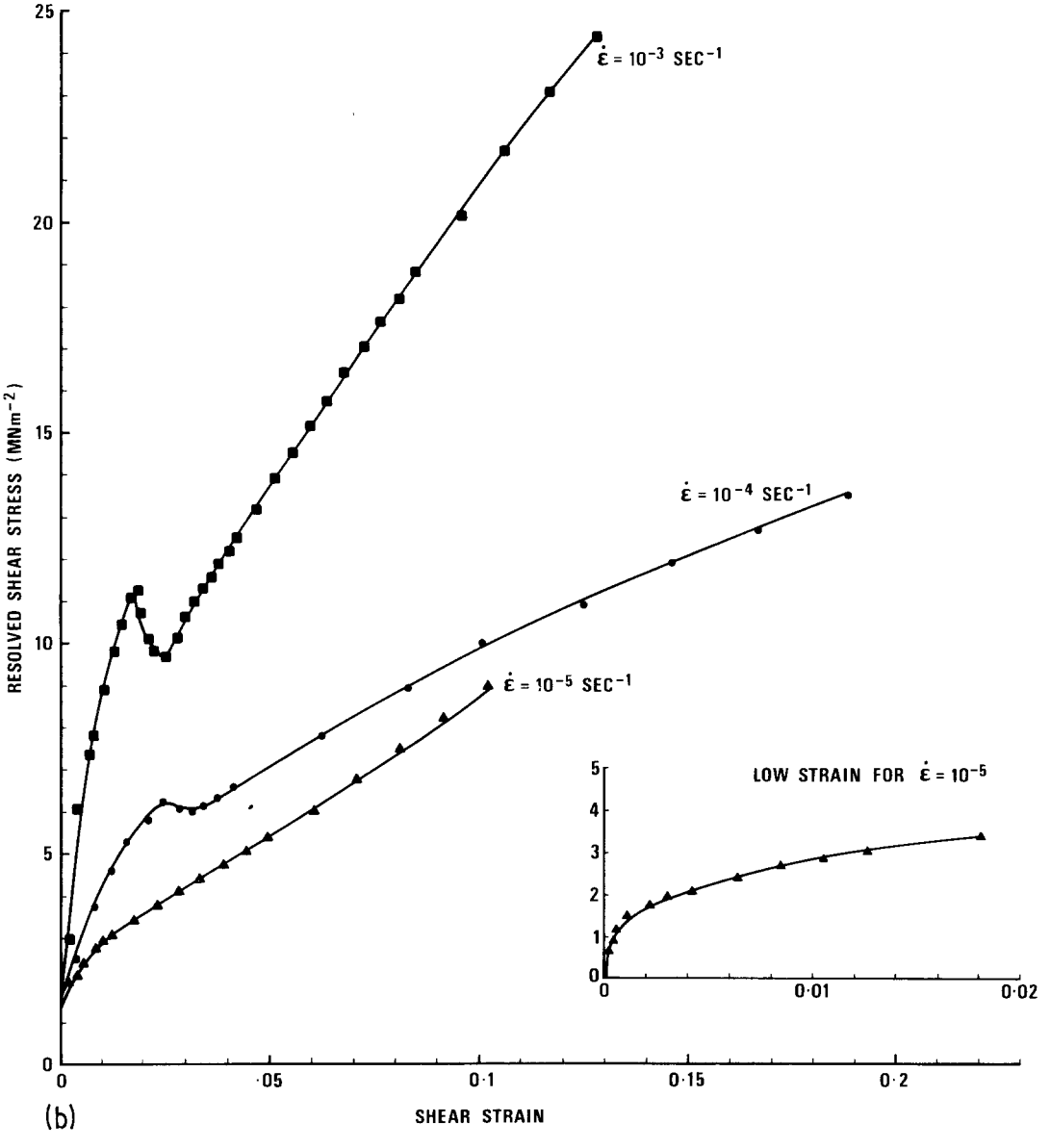

1. The situation can be described by the expression, [11],

$$\dot{\epsilon} = v\rho b,$$

where $\dot{\epsilon}$ is the strain rate, v, the average velocity of dislocations, ρ, the dislocation density and b, the Burgers vector. For a dislocation density which is initially low, a high strain rate can only be accommodated by a high dislocation velocity which requires a larger applied stress, but as soon as the density starts to increase due to normal dislocation multiplication processes, a load drop can occur and the magnitude of this drop is obviously greatest at the highest strain rate.

Three further points arise from Fig. 1 which require explanation. Firstly comparisons of the magnitude of the upper yield points for the two orientations show that a much greater upper yield stress is attained for the single slip orientation. This may be understood in terms of a more rapid increase in dislocation density with stress, prior to the upper yield point, for the multiple slip orientation, ⟨1 0 0⟩. Secondly, the less pronounced load drops observed for the ⟨0 0 1⟩ orientation were associated with a more rapid increase in dislocation density than experienced for the ⟨1 2 3⟩ orientation, due to multiple slip. Thirdly, the discontinuities present in the curve for the ⟨1 2 3⟩

sample at a strain rate of $10^{-3}\,sec^{-1}$ are unexplained but could be associated with buckling observed in this specimen.

3.2. The effect of temperature on deformation behaviour

The deformation behaviour is tabulated as a function of homologous temperature in Table II. No plastic deformation was observed below 480° C ($0.56T_m$) and fracture usually propagated along the {0 1 1} planes, although fracture occasionally occurred on {1 1 1} planes. At temperatures within the range $0.56T_m$ to $0.75T_m$ (730° C) plastic deformation occurred by a combination of slip and twinning on a fine scale. The deformation

TABLE II The deformation behaviour of InP single crystals with temperature

Homologous temperature	Strain rate (sec^{-1})		
	10^{-3}	10^{-4}	10^{-5}
⟨1 0 0⟩ *deformation axis*			
0.56		F T S	F T S
0.61		F T S	F T S
0.64	F	F T S	F T S
0.67	F	F T S	
0.71	T S	T S	S
0.75	S	S	
⟨1 2 3⟩ *deformation axis*			
0.52		F	F
0.55	F	F T S	
0.59		F T S	T S
0.64	F	T S	S
0.67	T S	S	S
0.71	S	S	

F, deformation occurred by fracture or cracking.
T, deformation twinning was observed.
S, slip lines were observed.

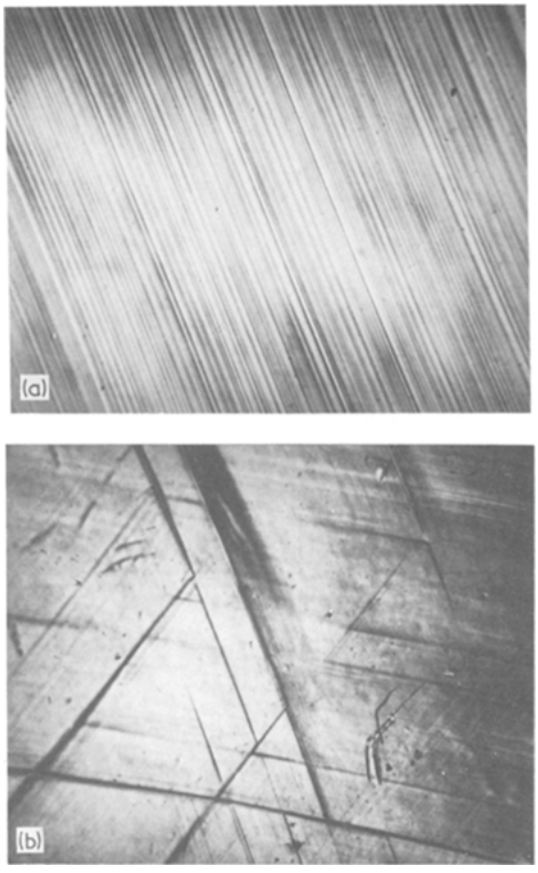

Figure 2 Optical micrographs imaged using Nomarski interference contrast at × 150 showing (a) fine slip on the {1 4 5} face of a ⟨1 2 3⟩ axis specimen deformed at $0.67T_m$ at $10^{-4}\,sec^{-1}$; (b) Deformation twins on the {1 1 0} face of a ⟨0 0 1⟩ axis specimen deformed at $0.61T_m$ at $10^{-5}\,sec^{-1}$.

bands observed on the specimen deformed in this temperature range were predominantly deformation twins but a small number were identified as slip bands. At the higher temperatures used, deformation occurred by slip alone, but the surfaces of specimens tested above 730° C showed excessive degradation with the formation of microscopic spheroids of indium formed by phosphorus loss [14]. The development of fine slip lines over the entire specimen length, which occurred for higher temperatures ($T > 0.7T_m$) is illustrated in Fig. 2a. Clearly, slip was easily nucleated at these temperatures and was observed on all four available slip planes for specimens with the ⟨0 0 1⟩ compression axis. For specimens deformed along the ⟨1 2 3⟩ axis, slip was generally confined to the primary slip plane although at higher strains, deformation bands were observed on the secondary slip system.

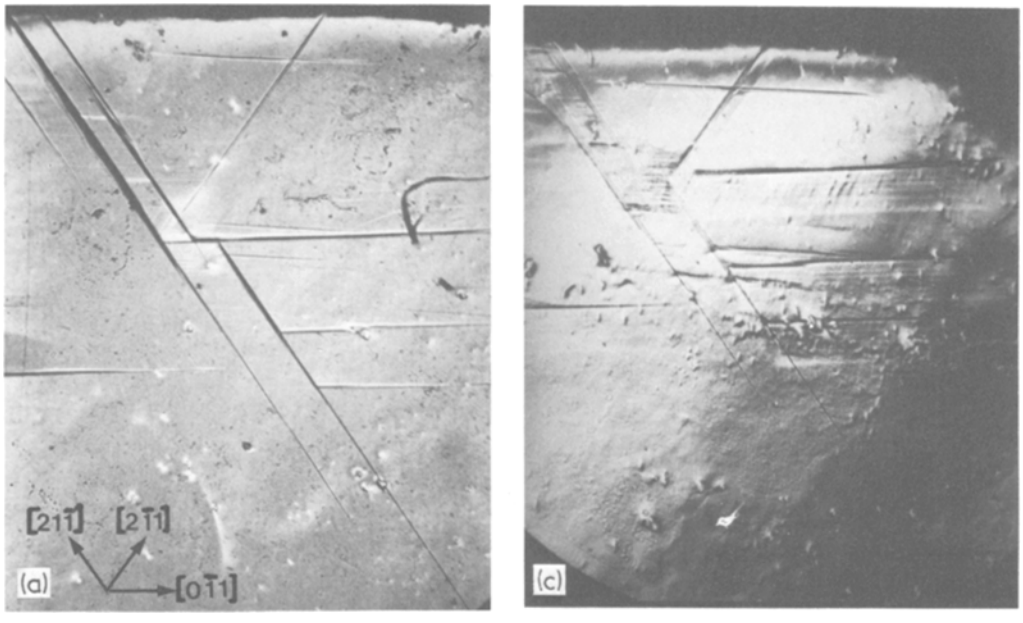

Figure 3 Optical micrographs imaged using Nomarski interference contrast at × 60 for a ⟨0 0 1⟩ axis specimen deformed at $0.56T_m$ at 10^{-5} sec^{-1}, (a) as-deformed, (b) above area chemically polished in a bromine–methanol solution, (c) above area etched in boiling 6:6:1 (HNO_3:H_2O:HCl).

At lower temperatures, slip was less homogeneously distributed and was accompanied by deformation bands (Fig. 2b). Direct optical examination gave insufficient information to differentiate the deformation bands as slip bands, microcracks or deformation twins, although interference fringe patterns showed that the bands were associated with a surface step of height $< 1\,\mu$m. The deformation bands were also too small for investigation by X-ray diffraction techniques and, hence, were examined using preferential etching and transmission electron microscopy. The bands could be polished away using a solution of a few percent bromine in methanol but reappeared after etching in a boiling acid mixture ($6HNO_3$: $6H_2O$: 1HCl). This sequence of events is shown in Fig. 3; Fig. 3a shows the (0 1 1) face of a [1 0 0] axis specimen where the emergence of bands along the [0 $\bar{1}$ 1], [2 $\bar{1}$ 1] and [2 1 $\bar{1}$] directions is evident. The reappearance of the bands after polishing and etching is shown in Fig. 3b and c. If these bands were slip lines they would not reappear, hence, they must be deformation twins and from their surface traces must lie on (1 1 1), (1 1 $\bar{1}$) and (1 $\bar{1}$ 1) planes, respectively. Fig. 3a and c also show twins with a surface trace at 8° to the [0 $\bar{1}$ 1] which is coincident with the emergence of the (5 3 4) plane along the [$\bar{1}$ $\bar{5}$ 5] direction at an angle of 8° to [0 $\bar{1}$ 1]. No {1 2 3} or {1 1 1} planes emerge along this direction.

The specimen illustrated in Fig. 3 was thinned for transmission electron microscopy and one of the bands along the [2 1 $\bar{1}$] direction transected the thin area. Fig. 4a and b are the bright-field micrographs of this area whilst the selected-area diffraction patterns from the matrix and from the matrix plus twin are shown in Figs. 5a and b,

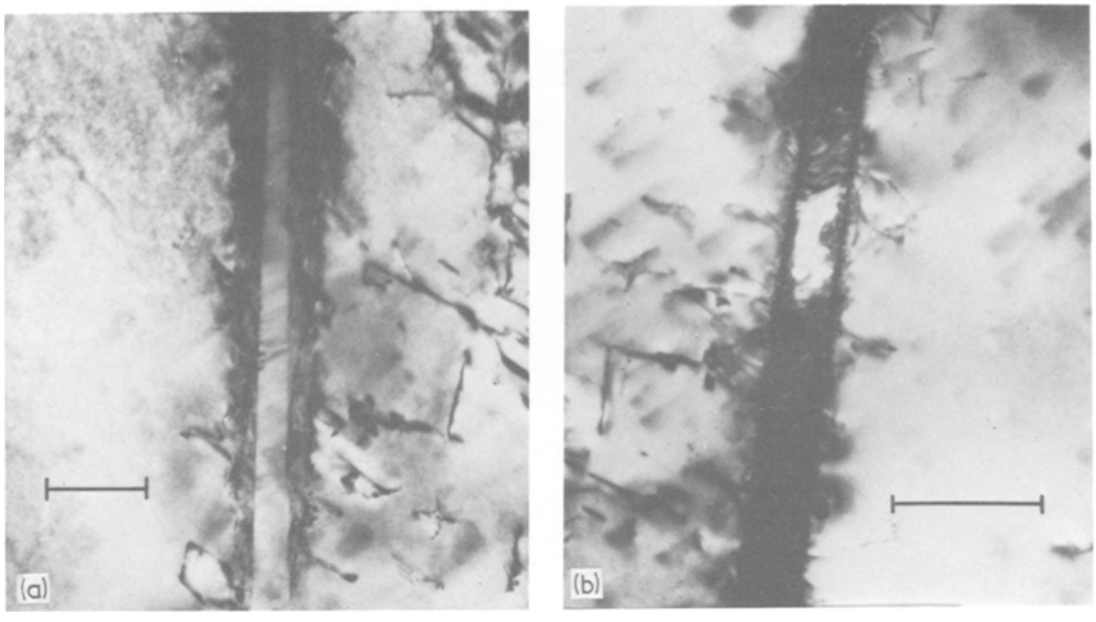

Figure 4 (a) and (b) are bright-field transmission electron micrograph taken on the HVEM. The magnification markers correspond to 0.5 μm.

respectively. The foil orientation is [0 1 1] and both twin and matrix give ⟨0 1 1⟩ diffraction patterns which are rotated relative to each other by 73°. For a perfect twin orientation relationship with a (1 $\bar{1}$ 1) twin plane parallel to the beam direction, the relative rotation should be 70.5°. This 2.5° deviation from the perfect twin orientation relationship can be seen very clearly in the comparison of [1 $\bar{1}$ 1] reflections for twin and matrix (Fig. 5b). One possible explanation for this slight deviation from a perfect twin orientation relationship is that a low-angle boundary has been superimposed on the twin boundary as a result of climb by some of the dislocations which have piled up in the vicinity of the twin as shown in Fig. 4a; dislocation climb is quite feasible at the deformation temperature of $0.56T_m$ for this sample. An alternative explanation is that the elastic strain

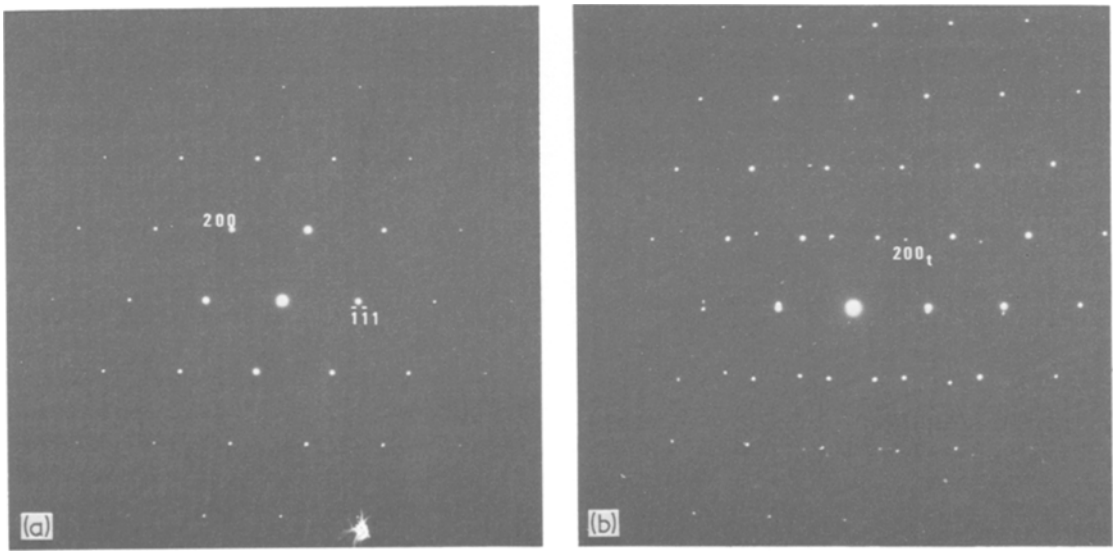

Figure 5 (a) Electron diffraction pattern from the matrix. (b) Electron diffraction pattern from the matrix and twin. Both of these were taken on the JEOL-100C electron microscope.

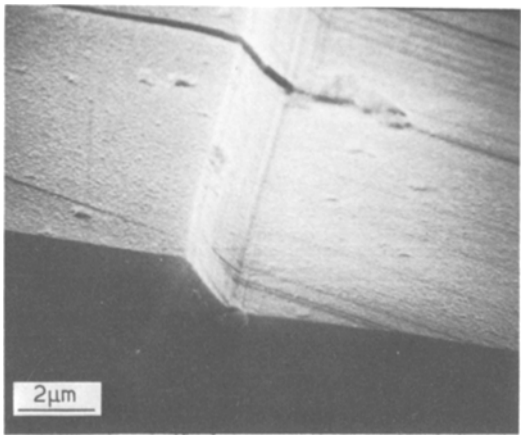

Figure 6 Scanning electron micrographs of the {111}P face of a ⟨123⟩ specimen deformed at $0.55T_m$ at 10^{-4} sec^{-1} showing the emergence of a deformation twin at a crack.

associated with a high dislocation density at the boundary may have caused a localized tilt across the twin.

Fig. 4b shows that considerable slip has occurred within the deformation twin and this explains the fine structure observed within the twin bands revealed by scanning electron microscopy (Fig. 6).

3.3. Deformation twinning in InP

The occurrence of deformation twins in InP observed here on {111} planes, has not been reported previously and, as far as the authors are aware, this is also the first observation of deformation twinning on the {345} planes in the diamond or sphalerite structure, although the {345} planes can theoretically constitute a twinning plane [15]. Fine-scale deformation twinning obviously occurs relatively easily in InP and the fine scale is probably responsible for the absence of the large load drops which normally accompany macroscopic twinning, for instance, in metals such as tin. The fine slip which occurs simultaneously with twinning also shows that the stress levels and temperature regimes required for twinning and slip are fairly similar.

3.4. Twins and dislocations in crystal growth

It has been suggested that the extreme thermal conditions experienced by the growing crystal in LEC growth may lead to deformation twins being propagated back to the growth interface. The results show that twinning only occurred between $0.56T_m$ and $0.75T_m$ under uniaxial compression. The pressures in the crystal pulling chamber (approximately 3 MN m^{-2} (30 atm)) superimpose a hydrostatic compression on the shear stresses produced by non-uniform cooling rates within the grown crystal. This is, however, highly unlikely to be high enough to influence the deformation behaviour. The temperature just above the boric oxide layer falls sharply from the boric oxide surface up towards the seed, falling from 850° C ($0.84T_m$) to 625° C ($0.67T_m$) in 0.5 cm s [13]. Deformation twinning could therefore be nucleated in this region of the grown crystal (i.e. up to 0.5 cm above the boric oxide). Observations of crystal growth made in these laboratories have concluded that the initial twins become visible before they emerge from the boric oxide. These twins must therefore nucleate at or near to the growth interface where the temperature is close to 1000° C and clearly this is a regime where deformation twinning cannot occur. However, the role of deformation in the formation of subsequent twins is not so readily assessed.

The ductile behaviour of InP at low strain rates and low temperature ($0.56T_m = 480°$ C) clearly implies that dislocations may be generated easily under the hoop stresses experienced during Czochralski growth. Again, this applies particularly to the region where the crystal emerges from the boric oxide encapsulant where both the radial and vertical temperature gradients are enhanced.

4. Conclusions

The deformation behaviour of InP has been shown to be a sensitive function of strain rate and temperature. The ductile-to-brittle transition is obviously a function of strain rate but ductile behaviour is prevalent above $0.7T_m$ at strain rates lower than 10^{-3} sec^{-1}. At temperatures within the range 0.55 to $0.71T_m$ deformation is shown to occur by both slip and twinning; above $0.71T_m$ slip alone is the operative mechanism.

Deformation twinning has been shown to occur readily in uniaxial compression and twins have been identified on {111} planes and in one instance on the {345} plane.

Acknowledgements

The authors would like to thank Mr D. G. Coates for his assistance with the scanning electron microscopy, and Dr A. G. Cullis for his assistance with transmission electron microscopy. The availability

of the HVEM at Birmingham University is also greatly appreciated.

References

1. D. LAISTER and G. M. JENKINS, *J. Mater. Sci.* 8 (1973) 1218.
2. U. BAITINGER, J. ARNDT and D. SCHNEPF, *ibid* **4** (1969) 396.
3. R. L. BELL, R. LAKOWSKI and A. F. W. WILLOUGHBY, *ibid* **1** (1966) 66.
4. H. SHIMIZU and K. SUMINO, *Phil. Mag.* **32** (1975) 123.
5. D. B. HOLT, *J. Phys. Chem. Solids* **23** (1962) 1353.
6. H. GOTTSCHALK, G. PATZER and H. ALEXANDER, *Phys. Stat. Sol.* (*a*) **45** (1978) 207.
7. A. T. CHURCHMAN, G. A. GEACH and J. WINTON, *Proc. Roy. Soc.* **A238** (1956) 194.
8. F. L. EDEL'MAN, *Sov. Phys. Solid State* 9 (1968) 1648.
9. W. BARDSLEY, G. W. GREEN, C. H. HALLIDAY and D. T. J. HURLE, *J. Crystal Growth* **16** (1972) 277.
10. R. C. CLARKE, D. S. ROBERTSON and A. W. VERE, *J. Mater. Sci.* 8 (1973) 1349.
11. W. G. JOHNSTON and J. J. GILMAN, *J. Appl. Phys.* **30** (1959) 129.
12. A. H. COTTRELL, "Dislocations and Plastic Flow in Crystal" (Oxford University Press, Oxford, 1953) p. 139.
13. K. J. BACHMAN, E. BUEHLER, J. L. SHAY and A. R. STNAD, *J. Electronic Mater.* 4 (1975) 389.
14. R. F. C. FARROW, *J. Phys. D Appl. Phys.* 8 (1975) L87.
15. R. BULLOUGH, *Proc. Roy. Soc.* **A341** (1957) 568.

Received 28 February and accepted 5 November 1979.